

Branching ratio and CP asymmetry for $B \rightarrow 1^1P_1\gamma$ decays

M. Jamil Aslam*

National Centre for Physics and Department of Physics, Quaid-i-Azam University, Islamabad, Pakistan

Riazuddin

National Centre for Physics, Quaid-i-Azam University, Islamabad, Pakistan.

(Received 20 July 2006; revised manuscript received 11 December 2006; published 7 February 2007)

We calculate the branching ratios for $B \rightarrow (b_1, h_1)\gamma$ at next-to-leading order (NLO) of α_s where b_1 and h_1 are the corresponding orbitally excited axial vector mesons of ρ and ω respectively. Using the $SU(3)$ symmetry for the form factors, the branching ratio for $B \rightarrow (b_1, h_1)\gamma$ is expressed in terms of the branching ratio of the $B \rightarrow K_1\gamma$ and it is found to be $\mathcal{B}(B \rightarrow b_1\gamma) = 0.53 \times 10^{-6}$ and $\mathcal{B}(B \rightarrow h_1\gamma) = 0.51 \times 10^{-6}$. We also calculate direct CP -asymmetry for these decays and find that its typical values lies around 11% and is negative like ρ and ω in the standard model. The predicted value of CP -asymmetry, in conformity with the observations made in the literature, is scale dependent which has also been discussed in detail.

DOI: [10.1103/PhysRevD.75.034004](https://doi.org/10.1103/PhysRevD.75.034004)

PACS numbers: 13.20.He, 12.38.Bx

I. INTRODUCTION

The Flavor-Changing-Neutral-Current (FCNC) processes which cause $b \rightarrow s\gamma$ and $b \rightarrow d\gamma$ decays may contain new physics (NP) effects through penguin amplitudes. As the SM effects represent the background when we search for NP effects, we shall compute these effects. In doing so, we can understand the sensitivity of each NP search.

The first experimental evidence of this FCNC transition process in B decay was observed about a decade ago, where the inclusive process $b \rightarrow s\gamma$ and exclusive process $B \rightarrow K^*\gamma$ were detected, and their branching ratios were measured [1,2]. On the other hand, the expected branching ratio for $b \rightarrow d\gamma$ is suppressed by $\mathcal{O}(10^{-2})$ with respect to the $b \rightarrow s\gamma$, because of the Cabbibo-Kobayashi-Masukawa quark mixing matrix factor (CKM). The world average for $b \rightarrow d$ penguin decays are given as follows: [3]

$$\begin{aligned}\mathcal{B}(B \rightarrow \rho^0\gamma) &= (0.38 \pm 0.18) \times 10^{-6} \\ \mathcal{B}(B \rightarrow \omega\gamma) &= (0.54_{-0.21}^{+0.23}) \times 10^{-6} \\ \mathcal{B}(B^+ \rightarrow \rho^+\gamma) &= (0.68_{-0.31}^{+0.36}) \times 10^{-6}.\end{aligned}\quad (1)$$

Theoretically, $B \rightarrow (\rho, \omega)\gamma$ are widely studied both within and beyond the SM [4,5]. Now after the first measurement of BELLE for the decay $B \rightarrow K_1\gamma$, where K_1 are the higher resonances of kaon [6], these higher states become a subject of topical interest for the theoreticians. These decays have been studied widely in the literature [7–10]. Recently, the leading-twist LCDAs as well as the first few Gegenbauer moments of 1^1P_1 mesons, $b_1(1235)$ and $h_1(1170)$, which are the axial vector states of the ρ and ω mesons have been studied [11]. It is pointed out that these LCDAs are not only important to explore the tensor-type new-physics in B decays but also for $B \rightarrow 1^1P_1\gamma$ studies.

In this paper the branching ratios for $B \rightarrow (b_1, h_1)\gamma$ at NLO of α_s are calculated using the LEET approach [12,13]. We follow the same frame work as was done by Ali *et al.* [14] for $B \rightarrow (\rho, \omega)\gamma$, because $B \rightarrow (b_1, h_1)\gamma$ shares many things with it. The only difference is the DA for the daughter meson. As b_1 and h_1 are axial vectors and are distinguished from vectors by the γ_5 in the gamma structure of DA and some non perturbative parameters. But the presence of γ_5 does not alter the calculation, give the same result for the perturbative part. The higher twist terms are also included through the Gegenbauer moments in the Gegenbauer expansion.

At next-to-leading order of α_s , $B \rightarrow (\rho, \omega)\gamma$ and $B \rightarrow (b_1, h_1)\gamma$ are characterized by the weak form factor and decay constant, plugged by the common perturbative and kinematical factors. With $\mathcal{B}(B \rightarrow (\rho, \omega)\gamma)$ at hand, we can say that the future experiment will check the structure for $B \rightarrow (b_1, h_1)\gamma$.

The paper is organized as follows. In Sec. II we will discuss the theoretical frame work for $B \rightarrow 1^1P_1\gamma$ decays whereas the Sec. III deals with the calculation of hard-spectator contributions to the said decays. By using the analytical results derived in this section we will calculate the branching ratio and discuss its dependence on the form factor, the only unknown quantity in our calculation, in the same section. In Sec. IV we will describe how one can calculate the CP -asymmetry for these decays and we also discuss its dependence on different scales. We will summarize our results at the end.

II. THEORETICAL FRAMEWORK FOR THE $B \rightarrow 1^1P_1\gamma$ DECAYS

The effective Hamiltonian for the radiative $b \rightarrow d\gamma$ decays (equivalently $B \rightarrow b_1\gamma$ and $B \rightarrow h_1\gamma$ decays) is obtained from the standard model (SM) by integrating out the heavy degrees of freedom (the top quark and

*Electronic address: jamil@ncp.edu.pk

$\mathcal{H}_{\text{eff}}^{b \rightarrow d}$ bosons). The resulting expression at the scale $\mu = O(m_b)$, where m_b is the b -quark mass, is given by

$$\begin{aligned} \mathcal{H}_{\text{eff}}^{b \rightarrow d} = & \frac{G_F}{\sqrt{2}} \{ V_{ub} V_{ud}^* [C_1^{(u)}(\mu) \mathcal{O}_1^{(u)}(\mu) + C_2^{(u)}(\mu) \mathcal{O}_2^{(u)}(\mu)] \\ & + V_{cb} V_{cd}^* [C_1^{(c)}(\mu) \mathcal{O}_1^{(c)}(\mu) + C_2^{(c)}(\mu) \mathcal{O}_2^{(c)}(\mu)] \\ & - V_{tb} V_{td}^* [C_7^{\text{eff}}(\mu) \mathcal{O}_7(\mu) + C_8^{\text{eff}}(\mu) \mathcal{O}_8(\mu)] + \dots \}, \end{aligned} \quad (2)$$

where G_F is the Fermi coupling constant and only the dominant terms are shown. The operators $\mathcal{O}_1^{(q)}$ and $\mathcal{O}_2^{(q)}$, ($q = u, c$), are the standard four-fermion operators and \mathcal{O}_7 and \mathcal{O}_8 are the electromagnetic and chromomagnetic penguin operators, respectively. Their explicit expressions are

$$\begin{aligned} \mathcal{O}_1^{(q)} &= (\bar{d}_\alpha \gamma_\mu (1 - \gamma_5) q_\beta) (\bar{q}_\beta \gamma^\mu (1 - \gamma_5) b_\alpha), \\ \mathcal{O}_2^{(q)} &= (\bar{d}_\alpha \gamma_\mu (1 - \gamma_5) q_\alpha) (\bar{q}_\beta \gamma^\mu (1 - \gamma_5) b_\beta), \end{aligned} \quad (3)$$

$$\begin{aligned} \mathcal{O}_7 &= \frac{e m_b}{8\pi^2} (\bar{d}_\alpha \sigma^{\mu\nu} (1 + \gamma_5) b_\alpha) F_{\mu\nu}, \\ \mathcal{O}_8 &= \frac{g_s m_b}{8\pi^2} (\bar{d}_\alpha \sigma^{\mu\nu} (1 + \gamma_5) T_{\alpha\beta}^a b_\beta) G_{\mu\nu}^a. \end{aligned} \quad (4)$$

Here, e and g_s are the electric and color charges, $F_{\mu\nu}$ and $G_{\mu\nu}^a$ are the electromagnetic and gluonic field strength tensors, respectively, $T_{\alpha\beta}^a$ are the color $SU(N_c)$ group generators, and the quark color indices α and β and gluonic color index a are written explicitly. Note that in the operators \mathcal{O}_7 and \mathcal{O}_8 the d -quark mass contributions are negligible and therefore omitted. The coefficients $C_1^{(q)}(\mu)$ and $C_2^{(q)}(\mu)$ in Eq. (2) are the usual Wilson coefficients corresponding to the operators $\mathcal{O}_1^{(q)}$ and $\mathcal{O}_2^{(q)}$, while the coefficients $C_7^{\text{eff}}(\mu)$ and $C_8^{\text{eff}}(\mu)$ include also the effects of the QCD penguin four-fermion operators which are assumed to be present in the effective Hamiltonian (2) and denoted by ellipses there. For details and numerical values of these coefficients, see Ref. [15] and also references therein. We use the standard Bjorken-Drell convention [16] for the metric and the Dirac matrices; in particular $\gamma_5 = i\gamma^0\gamma^1\gamma^2\gamma^3$, and the totally antisymmetric Levi-Civita tensor $\varepsilon_{\mu\nu\rho\sigma}$ is defined as $\varepsilon_{0123} = +1$. A point to note is that the three CKM factors shown in $\mathcal{H}_{\text{eff}}^{b \rightarrow d}$ are of the same order of magnitude and, hence, the matrix elements in the decays $b \rightarrow d\gamma$ and $B \rightarrow (b_1, h_1)\gamma$ have non-trivial dependence on the CKM parameters. This is contrary to the case of $b \rightarrow s\gamma$ decay (equivalently the $B \rightarrow K_1\gamma$ decays), where among the three CKM factors $V_{qb}V_{qd}^* \rightarrow V_{qb}V_{qs}^*$ ($q = u, c, t$) appearing in the effective Hamiltonian $\mathcal{H}_{\text{eff}}^{b \rightarrow s}$, the combination $V_{ub}V_{us}^*$ is CKM suppressed, the corresponding contributions to the decay amplitude can be safely neglected.

What we need to calculate are the matrix elements $\langle 1^1P_1\gamma | \mathcal{H}_{\text{eff}}^{b \rightarrow d} | B \rangle$, where $\mathcal{H}_{\text{eff}}^{b \rightarrow d}$ is given in Eq. (2). At leading order in α_s , this involves only the operators \mathcal{O}_7 ,

$\mathcal{O}_1^{(u)}$ and $\mathcal{O}_2^{(u)}$. The contribution from \mathcal{O}_7 is termed as the long-distance contribution characterized by the top quark induced amplitude, where $\mathcal{O}_1^{(u)}$ and $\mathcal{O}_2^{(u)}$ corresponds to the short-distance contributions and it includes the penguin amplitude for the u and c quark intermediate states and also the so-called weak annihilation and W -exchange contributions. There is also some contribution from annihilation penguin diagrams, which, however, are small. The branching ratio has negligible dependence on these annihilation topologies but these are important if one wants to calculate the CP -asymmetry.

At next-to-leading order of α_s there are the contributions from the operators \mathcal{O}_2 and \mathcal{O}_8 along with that of the \mathcal{O}_7 in $B \rightarrow 1^1P_1\gamma$ decay. Each operator has its vertex contribution and hard-spectator contribution terms which we calculate explicitly. The detailed calculation of these hard-spectator contributions is given in [10,17] and the references there in.

III. MATRIX ELEMENTS AT NEXT-TO-LEADING ORDER OF $O(\alpha_s)$

A. Hard-spectator contribution

The Hard-spectator contribution is well described by the convolution between the hard kernel T_k and the light-cone distribution amplitudes of the involved mesons, Φ_B and $\Phi_{1^1P_1}$ and can be written as $\Phi_B \otimes T_k \otimes \Phi_{1^1P_1}$. The corresponding decay amplitude can be calculated in the form of convolution formula, whose leading term can be expressed as [17]

$$\Delta \mathcal{M}^{\text{(HSA)}} = \frac{4\pi\alpha_s C_F}{N_c} \int_0^1 du \int_0^\infty dl_+ M_{jk}^{(B)} M_{li}^{(1^1P_1)} \mathcal{T}_{ijkl}, \quad (5)$$

where N_c is the number of colors, $C_F = (N_c^2 - 1)/(2N_c)$ is the Casimir operator eigenvalue in the fundamental representation of the color $SU(N_c)$ group. The leading-twist two-particle light-cone projection operators $M_{jk}^{(B)}$ and $M_{li}^{(1^1P_1)}$ of B and 1^1P_1 mesons in the momentum representation are:

$$\begin{aligned} M_{jk}^{(B)} = & -\frac{if_B M}{4} \left[\frac{1 + \not{l}}{2} \left\{ \phi_+^{(B)}(l_+) \not{l}_+ \right. \right. \\ & \left. \left. + \phi_-^{(B)}(l_+) \left(\not{l}_- - l_+ \gamma_\perp^\mu \frac{\partial}{\partial l_\perp^\mu} \right) \right\} \gamma_5 \right]_{jk} \Big|_{l=(l_+/2)n_+}, \end{aligned} \quad (6)$$

$$\begin{aligned} M_{li}^{(1^1P_1)} = & -\frac{i}{4} \left[f_\perp^{(1^1P_1)} (\not{\epsilon}^* \not{l}) \gamma_5 \phi_\perp^{(1^1P_1)}(u) \right. \\ & \left. + f_\parallel^{(1^1P_1)} \left(\not{l} \frac{m}{E} (\not{v} \epsilon^*) \right) \gamma_5 \phi_\parallel^{(1^1P_1)}(u) \right]_{li}, \end{aligned} \quad (7)$$

where f_B is the B -meson decay constant, $f_\parallel^{(1^1P_1)}$ and $f_\perp^{(1^1P_1)}$

are the longitudinal and transverse 1^1P_1 -meson decay constants, respectively, and ε_μ is the 1^1P_1 -meson polarization vector. These projectors include also the leading-twist distribution amplitudes $\phi_+^{(B)}(l_+)$ and $\phi_-^{(B)}(l_+)$ of the B -meson and $\phi_{\parallel}^{(1^1P_1)}(u)$ and $\phi_{\perp}^{(1^1P_1)}(u)$ of the 1^1P_1 -meson. \mathcal{T}_{ijkl} is the hard-scattering amplitude. The Kinematical relations used to calculate the hard-spectator contributions are summarized as:

$$\begin{aligned} p_b^\mu &\simeq m_b v^\mu, & l^\mu &= \frac{l_+}{2} n_+^\mu + l_\perp^\mu + \frac{l_-}{2} n_-^\mu \\ k_1^\mu &\simeq u E n^\mu + k_\perp^\mu + O(k_\perp^2), \\ k_2^\mu &\simeq \bar{u} E n^\mu - k_\perp^\mu + O(k_\perp^2), & v^2 &= 1, \\ v^\mu &= (n_-^\mu + n_+^\mu)/2 & E &\simeq M/2 \\ q^\mu &= \omega n_+^\mu & \omega &= M/2 \end{aligned}$$

To calculate \mathcal{T}_{ijkl} let us consider the contribution from all the possible diagrams as done for the $B \rightarrow V\gamma$ [17].

1. Spectator corrections due to the electromagnetic dipole operator O_7

The corresponding diagrams are presented in Fig. 1 and the explicit expression is given by

$$\begin{aligned} \mathcal{T}_{ijkl}^{(1)} &= -i \frac{G_F}{\sqrt{2}} V_{td}^* V_{tb} C_7^{\text{eff}}(\mu) \frac{em_b(\mu)}{4\pi^2} \frac{[\gamma_\mu]_{kl}}{(l-k_2)^2} \\ &\times \left[(q\sigma e^*)(1+\gamma_5) \frac{\not{p}_b + \not{l} - \not{k}_2 + m_b}{(p_b + l - k_2)^2 - m_b^2} \gamma_\mu \right. \\ &\left. + \gamma_\mu \frac{\not{k}_1 + \not{k}_2 - \not{l}}{(k_1 + k_2 + l)^2} (q\sigma e^*)(1+\gamma_5) \right]_{ij} \end{aligned} \quad (8)$$

where the short-hand notation is used for $(q\sigma e^*) = \sigma^{\mu\nu} q_\mu e_\nu^*$.

2. Spectator corrections due to the chromomagnetic dipole operator O_8

The corresponding diagrams are presented in Fig. 2. The first two diagrams [Fig. 2(a)] show the corrections for the case when the photon is emitted from the flavor changing quark line and the result is

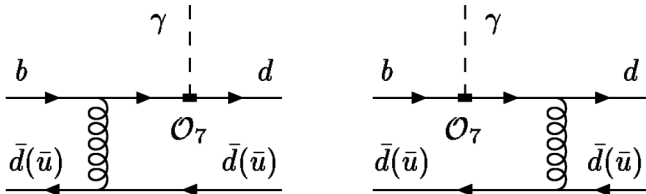


FIG. 1. Feynman diagrams contributing to the spectator corrections involving the O_7 operator in the decay $B \rightarrow 1^1P_1\gamma$. The curly (dashed) line here and in subsequent figures represents a gluon (photon).

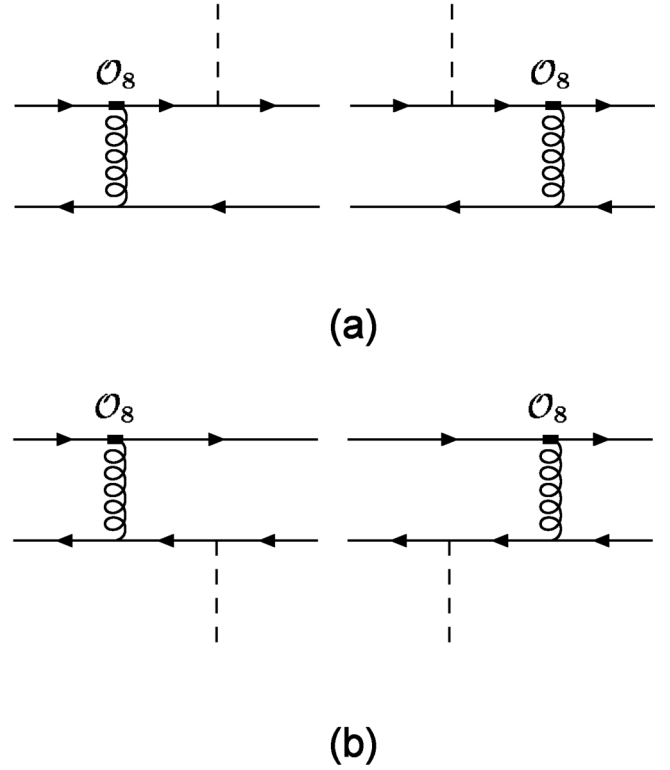


FIG. 2. Feynman diagrams contributing to the spectator corrections involving the O_8 operator in the decay $B \rightarrow 1^1P_1\gamma$. Row a: Photon is emitted from flavor changing quark line. Row b: Photon radiation off the spectator quark line.

$$\begin{aligned} \mathcal{T}_{ijkl}^{(2a)} &= -i \frac{G_F}{\sqrt{2}} V_{td}^* V_{tb} C_8^{\text{eff}}(\mu) \frac{em_b(\mu)}{4\pi^2} [\gamma_\nu]_{kl} \frac{(l-k_2)_\mu}{(l-k_2)^2} \\ &\times \left[\not{\epsilon}^* \frac{\not{p}_b + \not{l} - \not{k}_2}{(p_b + l - k_2)^2} \sigma_{\mu\nu} (1+\gamma_5) \right. \\ &\left. + \sigma_{\mu\nu} (1+\gamma_5) \frac{\not{k}_1 + \not{k}_2 - \not{l} + m_b}{(k_1 + k_2 + l)^2 - m_b^2} e^* \right]_{ij} \end{aligned} \quad (9)$$

Figure 2(b) contains the diagrams with the photon emission from the spectator quark which results into the following hard-scattering amplitude:

$$\begin{aligned} \mathcal{T}_{ijkl}^{(2b)} &= i \frac{G_F}{\sqrt{2}} V_{td}^* V_{tb} C_8^{\text{eff}}(\mu) \frac{eQ_{d[u]}m_b(\mu)}{4\pi^2} [\sigma_{\mu\nu}(1+\gamma_5)]_{ij} \\ &\times \frac{(p_b - k_1)_\mu}{(p_b - k_1)^2} \left[\gamma_\nu \frac{\not{p}_b + \not{l} - \not{k}_1}{(p_b + l - k_1)^2} \not{\epsilon}^* \right. \\ &\left. + \not{\epsilon}^* \frac{\not{k}_1 + \not{k}_2 - \not{p}_b}{(k_1 + k_2 - p_b)^2} \gamma_\nu \right]_{kl} \end{aligned} \quad (10)$$

where $Q_{d[u]}$ is the charge of the spectator quark.

3. Spectator corrections involving the penguin-type diagrams and the operator O_2

The corresponding diagrams are shown in Figs. 3–5. The hard-spectator contribution corresponding to the dia-

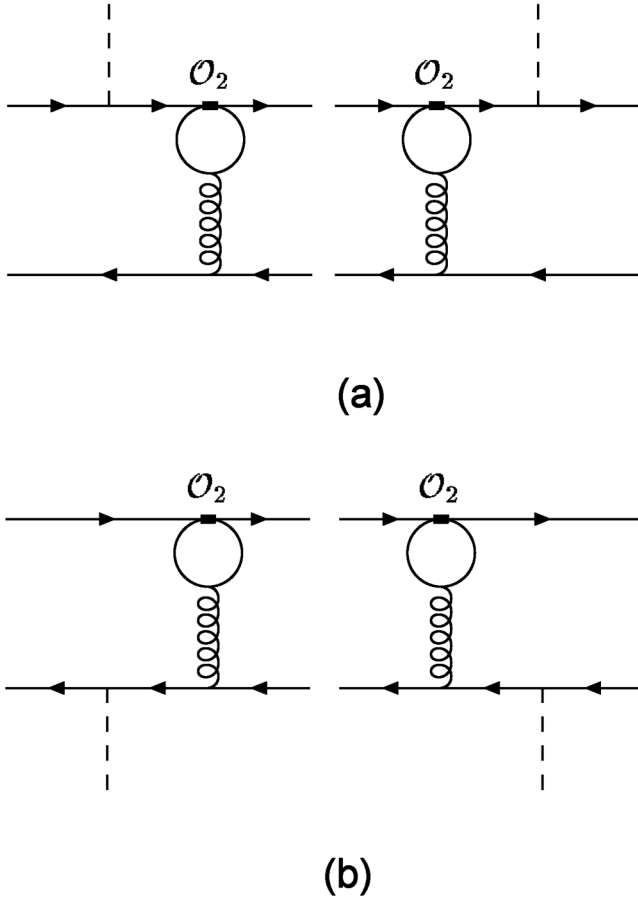


FIG. 3. Feynman diagrams contributing to the spectator corrections involving the O_2 operator in the decay $B \rightarrow 1^1P_1 \gamma$. Row a: Photon is emitted from flavor changing quark line. Row b: Photon radiation off the spectator quark line.

grams in Fig. 3(a) is

$$\begin{aligned}
\mathcal{T}_{ijkl}^{(3a)} &= \frac{G_F}{\sqrt{2}} \frac{e}{24\pi^2} \sum_{f=u,c} V_{fd}^* V_{fb} C_2^{(f)}(\mu) \Delta F_1(z_1^{(f)}) [\gamma_\nu]_{kl} \\
&\times \left[\left\{ \gamma_\nu - \frac{(k_2 - l)_\nu (k_2 - l)}{(k_2 - l)^2} \right\} (1 - \gamma_5) \right. \\
&\times \frac{\not{k}_1 + \not{k}_2 - \not{l} + m_b}{(k_1 + k_2 + l)^2 - m_b^2} \not{\epsilon}^* + \not{\epsilon}^* \frac{\not{p}_b + \not{l} - \not{k}_2}{(p_b + l - k_2)^2} \\
&\left. \times \left\{ \gamma_\nu - \frac{(k_2 - l)_\nu (k_2 - l)}{(k_2 - l)^2} \right\} (1 - \gamma_5) \right]_{ij} \quad (11)
\end{aligned}$$

$$\begin{aligned}
\mathcal{T}_{ijkl}^{(4)} &= -\frac{G_F}{\sqrt{2}} \frac{e}{6\pi^2} \frac{[\gamma_\nu]_{kl}}{(k_2 - l)^2 (q[k_2 - l])} \sum_{f=u,c} V_{fd}^* V_{fb} C_2^{(f)}(\mu) [\{ [q_\nu E(k_2 - l, e^*, q) - (q[k_2 - l]) E(\nu, e^*, q) \\
&+ (e^*[k_2 - l]) E(q, \nu, k_2 - l) - (q[k_2 - l]) E(e^*, \nu, k_2 - l)] \Delta i_5(z_0^{(f)}, z_1^{(f)}, 0) \\
&+ [(k_2 - l)^2 E(\nu, e^*, q) + (k_2 - l)_\nu E(e^*, k_2 - l, q)] \Delta i_{25}(z_0^{(f)}, z_1^{(f)}, 0) \} (1 - \gamma_5)]_{ij} \quad (13)
\end{aligned}$$

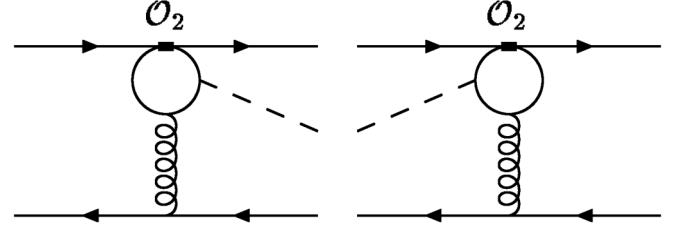


FIG. 4. Feynman diagrams contributing to the spectator corrections in $B \rightarrow 1^1P_1 \gamma$ decays involving the O_2 operator for the case when both the photon and the virtual gluon are emitted from the internal (loop) quark line.

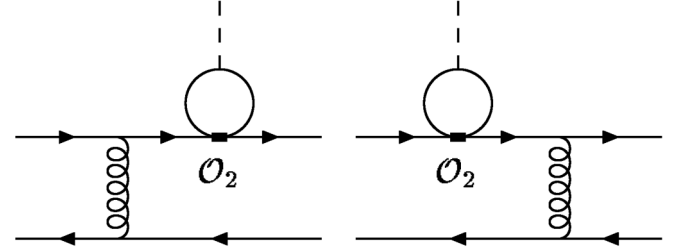


FIG. 5. Feynman diagrams contributing to the spectator corrections in $B \rightarrow 1^1P_1 \gamma$ decays involving the O_2 operator for the case when only the photon is emitted from the internal (loop) quark line in the $bd\gamma$ vertex.

and from the diagrams in Fig. 3(b), where the photon is emitted from the spectator quark line yield:

$$\begin{aligned}
\mathcal{T}_{ijkl}^{(3b)} &= \frac{G_F}{\sqrt{2}} \frac{e Q_d [u]}{24\pi^2} \sum_{f=u,c} V_{fd}^* V_{fb} C_2^{(f)}(\mu) \Delta F_1(z_0^{(f)}) \\
&\times \left[\not{\epsilon}^* \frac{\not{k}_1 + \not{k}_2 - \not{p}_b}{(k_1 + k_2 - p_b)^2} \gamma_\nu \right. \\
&+ \left. \gamma_\nu \frac{\not{p}_b + \not{l} - \not{k}_1}{(p_b + l - k_1)^2} \not{\epsilon}^* \right]_{kl} \\
&\times \left[\left\{ \gamma_\nu - \frac{(p_b - k_1)_\nu (p_b - k_1)}{(p_b - k_1)^2} \right\} (1 - \gamma_5) \right]_{ij} \quad (12)
\end{aligned}$$

The contributions from the diagrams in Fig. 4 can be written as

where

$$E(\mu, \nu, \rho) \equiv \frac{1}{2}(\gamma_\mu \gamma_\nu \gamma_\rho - \gamma_\rho \gamma_\nu \gamma_\mu) = -i\varepsilon_{\mu\nu\rho\sigma} \gamma^\sigma \gamma_5. \quad (14)$$

and the form of $\Delta F_1(z_1^{(f)})$, $\Delta F_1(z_0^{(f)})$, $\Delta i_5(z_0^{(f)}, z_1^{(f)}, 0)$ and $\Delta i_{25}(z_0^{(f)}, z_1^{(f)}, 0)$ along with the detailed discussion is given in [17].

Finally, there are the diagrams where the photon is emitted from the internal quark line due to the effective $b \rightarrow d\gamma$ interaction and a gluon is exchanged between the spectator quark and the b - or d quark as shown in Fig. 5. For on shell photon such kind of diagrams do not contribute and hence the contribution comes from the Fig. 5 is zero.

Using Eqs. (6) and (7) along with the hard-scattering matrix derived in the Eqs. (8)–(13) we can write from Eq. (5) as

$$\Delta \mathcal{M}_{\text{sp}}^{(1P_1)} = \frac{G_F}{\sqrt{2}} \frac{e\alpha_s C_F}{4\pi N_c} f_{B\perp}^{(1P_1)} M[(e^* \varepsilon^*) + i \text{eps}(e^*, \varepsilon^*, n_-, \nu)] \sum_{k=1}^5 \Delta H_k^{(1P_1)}, \quad (15)$$

where $\text{eps}(a, b, c, d) = \varepsilon_{\mu\nu\rho\sigma} a^\mu b^\nu c^\rho d^\sigma$ and the upper index 1^1P_1 characterizes the final axial meson. The dimensionless functions $\Delta H_k^{(1P_1)}$ ($k = 1, 2, 3, 4, 5$) describe the contributions of the sets of Feynman diagrams presented in Figs. 1–5, respectively. In the leading order of the inverse B -meson mass ($\sim \Lambda_{\text{QCD}}/M$), the result reads as follows:

$$\begin{aligned} \Delta \mathcal{M}_{\text{sp}} &= \frac{G_F}{\sqrt{2}} V_{tp}^* V_{tb} \frac{\alpha_s C_F}{4\pi} \frac{e}{4\pi^2} \Delta F_\perp^{(1P_1)}(\mu) [(pP)(e^* \varepsilon^*) + i \text{eps}(e^*, \varepsilon^*, p, P)] \\ &\times \left[C_7^{\text{eff}}(\mu) + \frac{1}{3} C_8^{\text{eff}}(\mu) \frac{\langle u^{-1} \rangle_\perp^{(1P_1)}}{\langle \bar{u}^{-1} \rangle_\perp^{(1P_1)}} + \frac{1}{3} C_2(\mu) \left(1 + \frac{V_{cd}^* V_{cb}}{V_{td}^* V_{tb}} \frac{h^{(1P_1)}(z, \mu)}{\langle \bar{u}^{-1} \rangle_\perp^{(1P_1)}(\mu)} \right) \right], \end{aligned} \quad (23)$$

where

$$\Delta F_\perp^{(1P_1)}(\mu) = \frac{8\pi^2 f_{B\perp}^{(1P_1)}(\mu)}{N_c M \lambda_{B,+}} \langle \bar{u}^{-1} \rangle_\perp^{(1P_1)}(\mu), \quad (24)$$

is the dimensionless quantity. $\lambda_{B,+}^{-1} = \langle l_+^{-1} \rangle_+$ is the first negative moment of the B -meson distribution function $\phi_+^{(B)}(l_+)$ and its scale dependence is worked out at next-to-leading order and the value obtained is $\lambda_{B,+}^{-1}(1 \text{ GeV}) = (2.15 \pm 0.50) \text{ GeV}$ [18]. At the scale $\mu_{\text{sp}} = \sqrt{\mu_b \Lambda_H}$ of the hard-spectator corrections, and for the central values of the parameters are shown in Table I.

The analytical expression for the function $h(z, \mu)$ for the vector meson is given in [17] and for the axial mesons is given in [10]. Here we will give some steps which are used to calculate these functions.

$$\begin{aligned} \Delta H_1^{(1P_1)}(\mu) &\simeq V_{td}^* V_{tb} C_7^{\text{eff}}(\mu) m_b(\mu) [\langle l_+^{-1} \rangle_+ \langle \bar{u}^{-1} \rangle_\perp^{(1P_1)}(\mu) \\ &+ \langle l_+^{-1} \rangle_- \langle \bar{u}^{-2} \rangle_\perp^{(1P_1)}(\mu)], \end{aligned} \quad (16)$$

$$\Delta H_2^{(1P_1)}(\mu) \simeq \frac{1}{3} V_{td}^* V_{tb} C_8^{\text{eff}}(\mu) m_b(\mu) \langle l_+^{-1} \rangle_+ \langle u^{-1} \rangle_\perp^{(1P_1)}(\mu), \quad (17)$$

$$\Delta H_3^{(1P_1)}(\mu) \simeq 0, \quad (18)$$

$$\begin{aligned} \Delta H_4^{(1P_1)}(\mu) &\simeq \frac{1}{3} C_2(\mu) M \langle l_+^{-1} \rangle_+ [V_{td}^* V_{tb} \langle \bar{u}^{-1} \rangle_\perp^{(1P_1)}(\mu) \\ &+ V_{cd}^* V_{cb} h^{(1P_1)}(z, \mu)], \end{aligned} \quad (19)$$

$$\Delta H_5^{(1P_1)}(\mu) \simeq 0, \quad (20)$$

where $z = m_c^2/m_b^2$ and the short-hand notation used are for the integrals over the mesons distribution functions:

$$\begin{aligned} \langle l_+^N \rangle_\pm &\equiv \int_0^\infty dl_+ l_+^N \phi_\pm^{(B)}(l_+), \\ \langle f \rangle_{\perp, \parallel}^{(1P_1)}(\mu) &\equiv \int_0^1 du f(u) \phi_{\perp, \parallel}^{(1P_1)}(u, \mu), \end{aligned} \quad (21)$$

with:

$$h^{(1P_1)}(z, \mu) = \left\langle \frac{\Delta i_5(z_0^{(c)}, 0, 0) + 1}{\bar{u}} \right\rangle_\perp^{(1P_1)}. \quad (22)$$

Using the above Equations one can write Eq. (15) as

One can write the leading-twist distribution amplitude $\phi_\perp^{(1P_1)}(u, \mu)$ as

$$\phi_\perp^{(1P_1)}(u, \mu) = 6u\bar{u} \left[1 + \sum_{n=1}^{\infty} a_{\perp n}^{(1P_1)}(\mu) C_n^{3/2}(u - \bar{u}) \right], \quad (25)$$

where $C_n^{3/2}(u - \bar{u})$ are the Gegenbauer polynomials [$C_1^{3/2}(u - \bar{u}) = 3(u - \bar{u})$, $C_2^{3/2}(u - \bar{u}) = 3[5(u - \bar{u})^2 - 1]/2$, etc.] and $a_{\perp n}^{(1P_1)}(\mu)$ are the corresponding Gegenbauer moments. These moments are scale dependent and so should be evaluated at the scale μ ; their scale dependence is governed by [19]:

TABLE I. Input quantities and their values used in the theoretical analysis.

Parameters	Values	Parameters	Values
M_W	80.423 GeV	M_Z	91.1876 GeV
M_B	5.279 GeV	m_{b_1}	1.229
G_F	1.166×10^{-5} GeV	m_{h_1}	1.170
$\alpha_s (M_Z)$	0.1172	α	1/137.036
$m_{t,\text{pole}}$	178 GeV	Λ_h	0.5 GeV
$ V_{ib}V_{td}^* $	5×10^{-3}	$m_{b,\text{pole}}$	4.27 GeV
f_B	200 MeV	$\sqrt{z} = m_c/m_b$	0.29
$a_{\perp 1}^{(b_1)}(1 \text{ GeV})$	0	$a_{\perp 2}^{(b_1)}(1 \text{ GeV})$	0.1
$a_{\perp 1}^{(h_1)}(1 \text{ GeV})$	0	$a_{\perp 2}^{(h_1)}(1 \text{ GeV})$	0.35
$f_{\perp}^{(b_1)}$	180 MeV	$f_{\perp}^{(h_1)}$	200 MeV
$\lambda_{B,+}^{-1}$	$(2.15 \pm 0.50) \text{ GeV}^{-1}$	$\sigma_{B,+}(1 \text{ GeV})$	1.4 ± 0.4

$$a_{\perp n}^{(1P_1)}(\mu) = \left(\frac{\alpha_s(\mu^2)}{\alpha_s(\mu_0^2)} \right)^{\gamma_n/\beta_0} a_{\perp n}^{(1P_1)}(\mu_0), \quad (26)$$

$$\gamma_n = 4C_F \left(\sum_{k=1}^n \frac{1}{k} - \frac{n}{n+1} \right),$$

where $\beta_0 = (11N_c - 2n_f)/3$ and γ_n is the one-loop anomalous dimension with $C_F = (N_c^2 - 1)/(2N_c) = 4/3$. In the limit $\mu \rightarrow \infty$ the Gegenbauer moments vanish, $a_{\perp n}^{(1P_1)}(\mu) \rightarrow 0$, and the leading-twist transverse distribution amplitude has its asymptotic form:

$$\phi_{\perp}^{(1P_1)}(u, \mu) \rightarrow \phi_{\perp}^{(\text{as})}(u) = 6u\bar{u}. \quad (27)$$

A simple model of the transverse distribution which includes contributions from the first $a_{\perp 1}^{(1P_1)}(\mu)$ and the second $a_{\perp 2}^{(1P_1)}(\mu)$ Gegenbauer moments only is used here in the analysis. In this approach the quantities $\langle u^{-1} \rangle_{\perp}^{(1P_1)}$ and $\langle \bar{u}^{-1} \rangle_{\perp}^{(1P_1)}$ are:

$$\langle u^{-1} \rangle_{\perp}^{(1P_1)} = 3[1 - a_{\perp 1}^{(1P_1)}(\mu) + a_{\perp 2}^{(1P_1)}(\mu)], \quad (28)$$

$$\langle \bar{u}^{-1} \rangle_{\perp}^{(1P_1)} = 3[1 + a_{\perp 1}^{(1P_1)}(\mu) + a_{\perp 2}^{(1P_1)}(\mu)],$$

and depend on the scale μ due to the coefficients $a_{\perp n}^{(1P_1)}(\mu)$. The LCDA for b_1 and h_1 meson has recently been calculated in [11]. The transverse decay constant of these mesons as well as the first few Gegenbauer moments of leading-twist LCDA are calculated by using QCD sum rule technique. The value of these Gegenbauer moments are summarized in Table I. The function $h^{(1P_1)}(z, \mu)$ introduced in Eq. (23) can be presented as an expansion on the Gegenbauer moments [10]:

$$h^{(1P_1)}(z, \mu) = h_0(z) + a_{\perp 1}^{(1P_1)}(\mu)h_1(z) + a_{\perp 2}^{(1P_1)}(\mu)h_2(z)$$

$$= [1 + 3a_{\perp 1}^{(1P_1)}(\mu) + 6a_{\perp 2}^{(1P_1)}(\mu)]$$

$$\times \langle (\Delta i_5 + 1)/\bar{u} \rangle_{\perp}^{(0)} - 6[a_{\perp 1}^{(1P_1)}(\mu)$$

$$+ 5a_{\perp 2}^{(1P_1)}(\mu)]\langle \Delta i_5 + 1 \rangle_{\perp}^{(0)} + 30a_{\perp 2}^{(1P_1)}(\mu)$$

$$\times \langle \bar{u}(\Delta i_5 + 1) \rangle_{\perp}^{(0)}, \quad (29)$$

where another short-hand notation is introduced for the integral:

$$\langle f(u) \rangle_{\perp}^{(0)} = \int_0^1 du f(u) \phi_{\perp}^{(\text{as})}(u). \quad (30)$$

The detail of relevant functions as well as the analytical form of the $\langle (\Delta i_5 + 1)/\bar{u} \rangle_{\perp}^{(0)}$, $\langle \Delta i_5 + 1 \rangle_{\perp}^{(0)}$ and $\langle \bar{u}(\Delta i_5 + 1) \rangle_{\perp}^{(0)}$ is given [17].

The amplitude (15) is proportional to the tensor decay constant $f_{\perp}^{(1P_1)}$ of the axial meson which is a scale dependent parameter. Their values at an arbitrary scale μ can be obtained with the help of the evolution equation [19]:

$$f_{\perp}^{(1P_1)}(\mu) = \left(\frac{\alpha_s(\mu^2)}{\alpha_s(\mu_0^2)} \right)^{4/(3\beta_0)} f_{\perp}^{(1P_1)}(\mu_0). \quad (31)$$

with the value of $f_{\perp}^{(1P_1)}(\mu_0)$ for b_1 and h_1 is given in the Table I.

4. Branching ratios

The branching ratio of the $B \rightarrow (b_1, h_1)$ decay corrected to $O(\alpha_s)$ can be written as follows [10]:

$$\begin{aligned}
\mathcal{B}_{\text{th}}(B \rightarrow 1^1 P_1 \gamma) &= \tau_B \Gamma_{\text{th}}(B \rightarrow 1^1 P_1 \gamma) \\
&= \tau_B \frac{G_F^2 \alpha |V_{tb} V_{td}^*|^2}{32\pi^4} m_{b,\text{pole}}^2 M^3 [\xi_{\perp}^{(1^1 P_1)}]^2 \\
&\quad \times \left(1 - \frac{m_{(1^1 P_1)}^2}{M^2}\right)^3 |C_7^{(0)\text{eff}} + A^{(1)}(\mu)|^2
\end{aligned} \tag{32}$$

where G_F is the Fermi coupling constant, $\alpha = \alpha(0) = 1/137$ is the fine-structure constant, $m_{b,\text{pole}}$ is the pole b -quark mass, M and $m_{(1^1 P_1)}$ are the B - and axial vector-meson masses, and τ_B is the lifetime of the B - or B^+ -meson. The value of these constants is used from [10,14] and are collected in Table I, for the numerical analysis. For this study, we consider $\xi_{\perp}^{(1^1 P_1)}$ as a free parameter and we will extract its value from the current experimental data on $B \rightarrow K_1 \gamma$ decays because K_1 is also an axial vector meson. This is in analogy with the calculation done for the branching ratio of $B \rightarrow (\rho, \omega) \gamma$ in terms of the branching ratio of $B \rightarrow K^* \gamma$ by Ali *et al.* [14].

The function $A^{(1)}$ in Eq. (32) can be decomposed into the following three components:

$$A^{(1)}(\mu) = A_{C_7}^{(1)}(\mu) + A_{\text{ver}}^{(1)}(\mu) + A_{\text{sp}}^{(1)1^1 P_1}(\mu_{\text{sp}}). \tag{33}$$

Here, $A_{C_7}^{(1)}$ and $A_{\text{ver}}^{(1)}$ are the $\mathcal{O}(\alpha_s)$ (i.e. NLO) corrections due to the Wilson coefficient C_7^{eff} and in the $b \rightarrow d\gamma$ vertex, respectively, and $A_{\text{sp}}^{(1)1^1 P_1}$ is the $\mathcal{O}(\alpha_s)$ hard-spectator corrections to the $B \rightarrow 1^1 P_1 \gamma$ amplitude and their explicit expressions are as follows:

$$A_{C_7}^{(1)}(\mu) = \frac{\alpha_s(\mu)}{4\pi} C_7^{(1)\text{eff}}(\mu), \tag{34}$$

$$\begin{aligned}
A_{\text{ver}}^{(1)}(\mu) &= \frac{\alpha_s(\mu)}{4\pi} \left\{ \frac{32}{81} [13C_2^{(0)}(\mu) + 27C_7^{(0)\text{eff}}(\mu) \right. \\
&\quad \left. - 9C_8^{(0)\text{eff}}(\mu)] \ln \frac{m_b}{\mu} - \frac{20}{3} C_7^{(0)\text{eff}}(\mu) \right. \\
&\quad \left. + \frac{4}{27} (33 - 2\pi^2 + 6\pi i) C_8^{(0)\text{eff}}(\mu) \right. \\
&\quad \left. + r_2(z) C_2^{(0)}(\mu) \right\},
\end{aligned} \tag{35}$$

$$\begin{aligned}
A_{\text{sp}}^{(1)1^1 P_1}(\mu_{\text{sp}}) &= \frac{\alpha_s(\mu_{\text{sp}})}{4\pi} \frac{2\Delta F_{\perp}^{(1^1 P_1)}(\mu_{\text{sp}})}{9\xi_{\perp}^{(1^1 P_1)}} \\
&\quad \times \left\{ 3C_7^{(0)\text{eff}}(\mu_{\text{sp}}) + C_8^{(0)\text{eff}}(\mu_{\text{sp}}) \right. \\
&\quad \times \left[1 - \frac{6a_{\perp 1}^{(1^1 P_1)}(\mu_{\text{sp}})}{\langle \bar{u}^{-1} \rangle_{\perp}^{(1^1 P_1)}(\mu_{\text{sp}})} \right] \\
&\quad \left. + C_2^{(0)}(\mu_{\text{sp}}) \left[1 + \frac{V_{cd}^* V_{cb}}{V_{td}^* V_{tb}} \frac{h^{(1^1 P_1)}(z, \mu_{\text{sp}})}{\langle \bar{u}^{-1} \rangle_{\perp}^{(1^1 P_1)}(\mu_{\text{sp}})} \right] \right\}.
\end{aligned} \tag{36}$$

Actually $C_7^{(1)\text{eff}}(\mu)$ and $A_{\text{ver}}^{(1)}(\mu)$ are process independent and encodes the QCD effects only, where as $A_{\text{sp}}^{(1)}(\mu_{\text{sp}})$ contains the key information about the outgoing mesons.

The factor $\frac{6a_{\perp 1}^{(1^1 P_1)}(\mu_{\text{sp}})}{\langle \bar{u}^{-1} \rangle_{\perp}^{(1^1 P_1)}(\mu_{\text{sp}})}$ appear in the Eq. (34) is arising due to the Gegenbauer moments. This term is zero for the case we are discussing here because the first Gegenbauer moment is zero.

We now proceed to calculate numerically the branching ratios for the $B \rightarrow b_1 \gamma$ and $B \rightarrow h_1 \gamma$ decays. The theoretical ratios involving the decay widths on the r.h.s. of these equations can be written in the form:

$$\begin{aligned}
R_{\text{th}}(b_1 \gamma / K_1 \gamma) &= \frac{\mathcal{B}_{\text{th}}(B \rightarrow b_1 \gamma)}{\mathcal{B}_{\text{th}}(B \rightarrow K_1 \gamma)} \\
&= \frac{1}{2} \left| \frac{V_{td}}{V_{ts}} \right|^2 \frac{(M_B^2 - m_{b_1}^2)^3}{(M_B^2 - m_{K_1}^2)^3} \\
&\quad \times \zeta^2 [1 + \Delta R(b_1 / K_1)],
\end{aligned} \tag{37}$$

$$\begin{aligned}
R_{\text{th}}(h_1 \gamma / K_1 \gamma) &= \frac{\bar{\mathcal{B}}_{\text{th}}(B \rightarrow h_1 \gamma)}{\bar{\mathcal{B}}_{\text{th}}(B \rightarrow K_1 \gamma)} \\
&= \frac{1}{2} \left| \frac{V_{td}}{V_{ts}} \right|^2 \frac{(M_B^2 - m_{h_1}^2)^3}{(M_B^2 - m_{K_1}^2)^3} \\
&\quad \times \zeta^2 [1 + \Delta R(h_1 / K_1)],
\end{aligned} \tag{38}$$

where m_{b_1} and m_{h_1} are the masses of the b_1 - and h_1 -mesons, ζ is the ratio of the transition form factors, which we have assumed to be the same for the b_1^0 - and h_1 -mesons. To get the theoretical branching ratios for the decays $B \rightarrow b_1 \gamma$ and $B \rightarrow h_1 \gamma$, the ratios (37) and (38) should be multiplied with the corresponding experimental branching ratio of the $B \rightarrow K_1 \gamma$ decay.

It is well known that in vector-meson case the theoretical uncertainty in the evaluation of the $R_{\text{th}}(\rho \gamma / K^* \gamma)$ and $R_{\text{th}}(\omega \gamma / K^* \gamma)$ ratios is dominated by the imprecise knowledge of $\zeta = \bar{T}_1^{\rho}(0) / \bar{T}_1^{K^*}(0)$ characterizing the $SU(3)$ breaking effects in the QCD transition form factors. In the

$SU(3)$ -symmetry limit, $\bar{T}_1^\rho(0) = \bar{T}_1^{K^*}(0)$, yielding $\zeta = 1$. We make use of the $SU(3)$ symmetry to relate the form factors of $B \rightarrow b_1\gamma$ and $B \rightarrow h_1\gamma$ with that of $B \rightarrow K_1\gamma$ decay which is the only unknown parameter involved in the calculation of branching ratio for these decays. We use this symmetry because there is no experimental limit on the branching ratio of these decays. It is reasonable to use $\xi_\perp^{1^1P_1}(0) = \xi_\perp^{K_1}(0)$ because $SU(3)$ symmetry is good for the form factors irrespective of the fact that it is not exact for the masses. Thus in present analysis we use $\xi_\perp^{1^1P_1}(0) = 0.32$ together with the values of the other input parameters entering in the calculation of the $B \rightarrow (b_1, h_1)\gamma$ decay amplitudes and these are given in Table I.

The individual branching ratios $\mathcal{B}_{\text{th}}(B \rightarrow b_1\gamma)$ and $\mathcal{B}_{\text{th}}(B \rightarrow h_1\gamma)$ and their ratios $\mathcal{R}_{\text{th}}(b_1\gamma/K_1\gamma)$ and $\mathcal{R}_{\text{th}}(h_1\gamma/K_1\gamma)$ with respect to the corresponding $B \rightarrow K_1\gamma$ branching ratios are calculated and the corresponding values are:

$$\mathcal{B}_{\text{th}}[B \rightarrow b_1\gamma] = 0.53 \times 10^{-6} \quad (39)$$

$$\mathcal{B}_{\text{th}}[B \rightarrow h_1\gamma] = 0.51 \times 10^{-6} \quad (40)$$

$$\mathcal{R}_{\text{th}}[b_1\gamma/K_1\gamma] = 0.0123 \quad (41)$$

$$\mathcal{R}_{\text{th}}[h_1\gamma/K_1\gamma] = 0.0121 \quad (42)$$

To calculate these values we have used the experimental value of the branching ratio of $B \rightarrow K_1\gamma$. One can easily see that there is very small difference between $B \rightarrow b_1\gamma$ and $B \rightarrow h_1\gamma$ branching fractions, and this is due to the slight change in the hadronic parameters of these decays. We will comment on these hadronic parameters in the next section where we will calculate the CP -asymmetry for these decays.

The $SU(3)$ -breaking effects in ρ and K^* form factors have been evaluated within several approaches, including

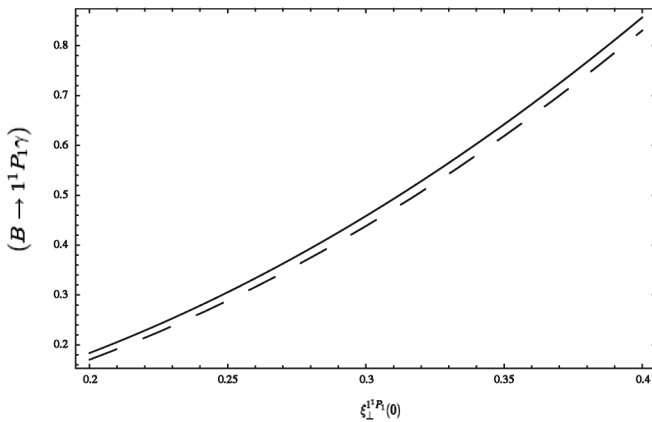


FIG. 6. Branching ratio ($\times 10^6$) for $B \rightarrow 1^1P_1\gamma$ decay vs LEET form factor; Solid line shows the value for b_1 meson and the dashed line is for h_1 meson.

the LCSR and Lattice QCD. In the earlier calculations of the ratios for $B \rightarrow \rho\gamma$ and $B \rightarrow K^*\gamma$ [17,20], the following ranges were used: $\zeta = 0.76 \pm 0.06$ [17] and $\zeta = 0.76 \pm 0.10$ [20], based on the LCSR approach [21–25] which indicate substantial $SU(3)$ breaking in the $B \rightarrow K^*$ form factors. There also exists an improved Lattice estimate of this quantity, $\zeta = 0.9 \pm 0.1$ [26]. To incorporate the $SU(3)$ symmetry for these axial meson decays we have plotted the branching ratios of $B \rightarrow (b_1, h_1)\gamma$ decay with the LEET form factor which is presented in Fig. 6. The solid and dashed line show the dependence of the branching ratio of $B \rightarrow b_1\gamma$ and $B \rightarrow h_1\gamma$ on the LEET form factor $\xi_\perp^{1^1P_1}(0)$ respectively. The graph shows that in the range $0.76 \leq \zeta \leq 0.9$ the value of the branching ratio (in the units of 10^{-6}) is $0.4 \leq (B \rightarrow 1^1P_1\gamma) \leq 0.7$.

IV. CP -VIOLATING ASYMMETRIES

In the last section we have calculated the branching ratio for $B \rightarrow 1^1P_1\gamma$ decays. We now present the effect of including hard-spectator corrections on the CP -asymmetries in the decay rates. It is pointed out in the literature that it is unlikely that the annihilation topology would give considerable contributions [9], but these are important if one wants to calculate the CP -asymmetries. As weak annihilation is a power correction, we will content ourselves to lowest order result ($\mathcal{O}(\alpha_s^0)$) for our estimate of CP -asymmetry. One may expect that power corrections, as they come with large Wilson coefficients $C_{1,2}$ ($C_1 \approx 3C_7$) are important, but infact they are not since these are CKM suppressed and thus these contributions are expected to be very small for the decays under consideration. The amplitude for charged B meson decay in terms of weak annihilation A , charmed penguin P_c , gluonic penguin M and short-distance amplitude P_t can be written as [following the notation of [27,28]]

$$\begin{aligned} A(B^- \rightarrow b_1^- \gamma) &= \lambda_t^{(d)} p \left(1 + \frac{\lambda_u^{(d)}}{\lambda_t^{(d)}} \frac{a}{p} \right) \\ &= \lambda_t^{(d)} p \left(1 + \epsilon_A e^{i\phi_A} \frac{\lambda_u^{(d)}}{\lambda_t^{(d)}} \right) \end{aligned}$$

where $\lambda_q^{(d)} = V_{qb} V_{qd}^*$, $a = A - P_c$ and $p = P_t + M - P_c$. As it is known [27]

$$P_c \simeq 0.2A, \quad A \simeq 0.3P_t$$

i.e. we can safely neglect charmed penguin P_c and gluonic penguin M (also is of the order of P_c) amplitudes relative to the short-distance amplitude P_t and weak annihilation amplitude A . Similarly,

$$A(B^0 \rightarrow b_1^0 \gamma) = \lambda_t^{(d)} p$$

where $\epsilon_A e^{i\phi_A} \equiv a/p$, ϕ_A is the strong interaction phase which disappears in $\mathcal{O}(\alpha_s)$ in the chiral limit. Hence we

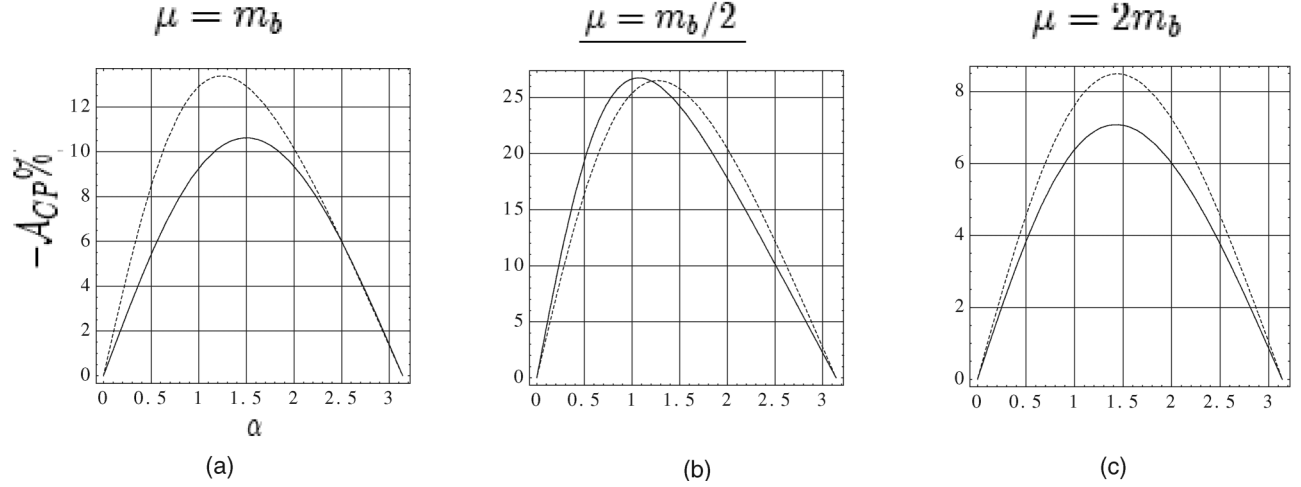


FIG. 7. CP -asymmetry ($-\mathcal{A}_{CP}\%$) vs the Unitarity-triangle phase α is plotted at different scales. Solid line is for b_1 meson and dashed line is for h_1 meson. Figs. 7(a)–7(c) and shows the corresponding value of CP -asymmetry at the scale $\mu = m_b, m_b/2$ and $2m_b$ respectively.

will set it equal to zero in the subsequent calculation. Following the same lines as for the charged B meson the ratio of the branching ratios for charged to neutral B meson decays can be written as

$$\frac{\mathcal{B}(B^- \rightarrow b_1^- \gamma)}{\mathcal{B}(B^0 \rightarrow b_1^0 \gamma)} \simeq \left| 1 + \epsilon_A e^{i\phi_A} \frac{V_{ub} V_{ud}^*}{V_{tb} V_{td}^*} \right|^2 \quad (43)$$

Before we go for the numerical values of CP -asymmetry, let us discuss the difference in the hadronic parameters involving the b_1 and h_1 mesons. As these are the axial vector states of ρ^0 and ω mesons so these are also the maximally mixed superpositions of the $\bar{u}u$ and $\bar{d}d$ quark states: $|b_1\rangle = (|\bar{d}d\rangle - |\bar{u}u\rangle)/\sqrt{2}$ and $|h_1\rangle = (|\bar{d}d\rangle + |\bar{u}u\rangle)/\sqrt{2}$. Neglecting the W -exchange contributions in the decays, the radiative decay widths are determined by the penguin amplitudes which involve only the $|\bar{d}d\rangle$ components of these mesons, leading to identical branching ratios (modulo a tiny phase space difference). The W -exchange diagrams from the $\mathcal{O}_1^{(u)}$ and $\mathcal{O}_2^{(u)}$ operators (in our approach, we are systematically neglecting the contributions from the penguin operators $\mathcal{O}_3, \dots, \mathcal{O}_6$) yield contributions equal in magnitude but opposite in signs [for detailed calculation please see [14,27]]. If we use the notations and expressions given in Ref. [27], the LCSR results are: $\epsilon_A^{(b_1)} = -\epsilon_A^{(h_1)} = 0.07$. The smallness of these numbers reflects both the color-suppressed nature of the W -exchange amplitudes in $B_d^0 \rightarrow (b_1, h_1)\gamma$ decays, and the observation that the leading contributions in the weak annihilation and W -exchange amplitudes arise from the radiation off the d -quark in the B_d^0 -meson, which is suppressed due to the electric charge. Let us defines

$$\frac{V_{ub} V_{ud}^*}{V_{tb} V_{td}^*} = - \left| \frac{V_{ub} V_{ud}^*}{V_{tb} V_{td}^*} \right| e^{i\alpha} = F_1 + iF_2 \quad (44)$$

where α is the unitarity-triangle phase.

Ignoring the hard-spectator corrections, but including the annihilation contribution, the result was given in [17]

$$\begin{aligned} \mathcal{B}_{\text{th}}(B^\pm \rightarrow b_1^\pm \gamma) &= \tau_B \Gamma_{\text{th}}(B^\pm \rightarrow b_1^\pm \gamma) \\ &= \tau_{B^+} \frac{G_F^2 \alpha^2 |V_{tb} V_{td}^*|^2}{32\pi^4} m_{b,\text{pole}}^2 M^3 \left(1 - \frac{m_{b_1}^2}{M^2}\right)^3 \\ &\quad \times [\xi_\perp^{(b_1)}(0)]^2 \{ (C_7^{(0)\text{eff}} + A_R^{(1)})^2 \\ &\quad + (F_1^2 + F_2^2)(A_R^u + L_R^u)^2 \\ &\quad + 2F_1 [C_7^{(0)\text{eff}}(A_R^u + L_R^u) + A_R^{(1)} L_R^u] \\ &\quad \mp 2F_2 [C_7^{(0)\text{eff}} A_L^u - A_L^{(1)} L_R^u] \}, \end{aligned} \quad (45)$$

with $L_R^u = \epsilon_A C_7^{(0)\text{eff}}$ and $A^{(1)}$ is same as defined in (33). The contribution from the u quark penguin can be written as

$$\begin{aligned} A^u(\mu) &= \frac{\alpha_s(\mu)}{4\pi} C_2^{(0)}(\mu) [r_2(z) - r_2(0)] \\ &\quad - \frac{\alpha_s(\mu_{\text{sp}})}{18\pi} C_2^{(0)}(\mu_{\text{sp}}) \frac{\Delta F_\perp^{(b_1)}(\mu_{\text{sp}})}{\xi_\perp^{(b_1)}(0)} \frac{h^{(b_1)}(z, \mu_{\text{sp}})}{\langle \bar{u}^{-1} \rangle_\perp^{(b_1)}(\mu_{\text{sp}})}. \end{aligned} \quad (46)$$

The direct CP -violating asymmetries in the decay rates for

TABLE II.

Scale	$\mathcal{A}_{CP}^{\text{dir}}(B_d^0 \rightarrow b_1 \gamma)$	$\mathcal{A}_{CP}^{\text{dir}}(B_d^0 \rightarrow h_1 \gamma)$
$\mu = m_b$	-11%	-13%
$\mu = m_b/2$	-25.5%	-25.5%
$\mu = 2m_b$	-7%	-9%

$B_d^0 \rightarrow (b_1, h_1)\gamma$ decays are defined as follows:

$$\begin{aligned}\mathcal{A}_{CP}^{\text{dir}}(b_1\gamma) &\equiv \frac{\mathcal{B}(\bar{B}_d^0 \rightarrow b_1\gamma) - \mathcal{B}(B_d^0 \rightarrow b_1\gamma)}{\mathcal{B}(\bar{B}_d^0 \rightarrow b_1\gamma) + \mathcal{B}(B_d^0 \rightarrow b_1\gamma)}, \\ \mathcal{A}_{CP}^{\text{dir}}(h_1\gamma) &\equiv \frac{\mathcal{B}(\bar{B}_d^0 \rightarrow h_1\gamma) - \mathcal{B}(B_d^0 \rightarrow h_1\gamma)}{\mathcal{B}(\bar{B}_d^0 \rightarrow h_1\gamma) + \mathcal{B}(B_d^0 \rightarrow h_1\gamma)}.\end{aligned}\quad (47)$$

Now by substituting the values of branching ratios calculated in Eq. (45) into the Eq. (47), the calculated values of the CP -asymmetry for the above mentioned decays are summarized in Table II. The CP -asymmetry receives contributions from the hard-spectator corrections which tend to decrease its value estimated from the vertex corrections alone. The dependence of the direct CP -asymmetry on the CKM unitarity-triangle angle α is presented in the Fig. 7 at different scales. It should be noted that the predicted direct CP -asymmetries are rather sizable (of order 11%) and is negative like ρ and ω meson case. It is quite unfortunate that the predicted value of CP -asymmetry is sensitive to both the choice of the scale as well as the quark mass ratio $z = m_c^2/m_b^2$ used in the calculation. In Table II we have calculated the dependence of CP -asymmetry on different scales. One can easily see that this asymmetry decreases with the increase of scale μ . This shows that the typical value lies around 11%, but the uncertainty is rather large and this increases to 25% at the scale $\mu = 2m_b$.

V. SUMMARY

We have calculated the branching ratios for $B \rightarrow 1^1P_1\gamma$ decays at NLO of α_s . These 1^1P_1 are b_1 and h_1 mesons

which are the corresponding orbitally excited axial vector mesons of ρ and ω respectively. Using the $SU(3)$ symmetry for the form factor, the branching ratio for $B_d^0 \rightarrow (b_1, h_1)\gamma$ is expressed in terms of the branching ratio of the $B_d^0 \rightarrow K_1\gamma$ and it is found to be $\mathcal{B}(B_d^0 \rightarrow b_1\gamma) = 0.53 \times 10^{-6}$ and $\mathcal{B}(B_d^0 \rightarrow h_1\gamma) = 0.51 \times 10^{-6}$. Then we have plotted the branching ratio with the LEET form factor which is the only unknown parameter involved in the calculation. It is shown that the corresponding to the range of $SU(3)$ symmetry breaking parameter ζ , $0.76 \leq \zeta \leq 0.9$ the value of the branching ratio (10^6) is $0.4 \leq (B_d^0 \rightarrow 1^1P_1\gamma) \leq 0.7$. Therefore in future when we have the experimental data on these decays we will be able to extract the value of form factor. Further we have also calculated direct CP -asymmetry for these decays and find, in conformity with the observations made in the literature, that this value is highly sensitive to the scale chosen. The typical value of CP -asymmetry is 11% and is negative like ρ and ω in the standard model. Thus the measurement of CP -asymmetry will either overconstrain the angle α of the unitarity triangle, or they may lead to the discovery of physics beyond the SM in the radiative $b \rightarrow d\gamma$ decays.

ACKNOWLEDGMENTS

One of the authors (J. A.) would like to thank Professor Fayyazuddin for valuable discussion. This work was supported by a grant from Higher Education Commission of Pakistan.

-
- [1] R. Ammar *et al.* (CLEO Collaboration), Phys. Rev. Lett. **71**, 674 (1993).
 - [2] M. S. Alam *et al.* (CLEO Collaboration), Phys. Rev. Lett. **74**, 2885 (1995).
 - [3] Heavy Flavor Averaging Group (HFAG), <http://www.slac.stanford.edu/xorg/hfag/>.
 - [4] C. Greub, H. Simma, and D. Wyler, Nucl. Phys. **B434**, 39 (1995); J. Milana, Phys. Rev. D **53**, 1403 (1996); A. Ali and V.M. Braun, Phys. Lett. B **359**, 223 (1995); J.F. Donoghue, E. Golowich, and A.A. Petrov, Phys. Rev. D **55**, 2657 (1997); T. Huang, Z.H. Li, and H.D. Zhang, J. Phys. G **25**, 1179 (1999); D. Pirjol, Phys. Lett. B **487**, 306 (2000); M. Beyer, D. Melikhov, N. Nikitin, and B. Stech, Phys. Rev. D **64**, 094006 (2001); S.W. Bosch, hep-ph/031031; M. Beneke, T. Feldmann, and D. Seidel, Eur. Phys. J. C **41**, 173 (2005).
 - [5] A. Ali, L.T. Handoko, and D. London, Phys. Rev. D **63**, 014014 (2000); L.T. Handoko, Nucl. Phys. B, Proc. Suppl. **93**, 296 (2001); A. Arhrib, C.K. Chua, and W.S. Hou, Eur. Phys. J. C **21**, 567 (2001); Z. Xiao and C. Zhuang, Eur. Phys. J. C **33**, 349 (2004); C.S. Kim, Y.G. Kim, and K.Y. Lee, hep-ph/0407060.
 - [6] K. Abe *et al.* (Belle Collaboration), hep-ex/0408138.
 - [7] A.S. Safir, Eur. Phys. J. C **3**, 15 (2001).
 - [8] Jong-Phil Lee, Phys. Rev. D **69**, 114007 (2004).
 - [9] Y.J. Kwon and Jong-Phil Lee, Phys. Rev. D **71**, 014009 (2005).
 - [10] M. Jamil Aslam and Riazuddin, Phys. Rev. D **72**, 094019 (2005).
 - [11] Kwei-Chou Yang, J. High Energy Phys. **10** (2005) 108.
 - [12] M.J. Dugan and B. Grinstein, Phys. Lett. B **255**, 583 (1991).
 - [13] J. Charles, A. Le Yaouanc, L. Oliver, O. Pene, and J.C. Raynal, Phys. Rev. D **60**, 014001 (1999).
 - [14] A. Ali, E. Lunghi, and A.Y. Parkhomenko, Phys. Lett. B **595**, 323 (2004).
 - [15] G. Buchalla, A.J. Buras, and M.E. Lautenbacher, Rev. Mod. Phys. **68**, 1125 (1996).
 - [16] J.D. Bjorken and S.D. Drell, *Relativistic Quantum Fields* (McGraw-Hill, New York, 1965).

- [17] A. Ali and A. Y. Parkhomenko, Eur. Phys. J. C **23**, 89 (2002).
- [18] V.M. Braun, D. Y. Ivanov, and G.P. Korchemsky, Phys. Rev. D **69**, 034014 (2004).
- [19] P. Ball, V.M. Braun, Y. Koike, and K. Tanaka, Nucl. Phys. **B529**, 323 (1998).
- [20] A. Ali and E. Lunghi, Eur. Phys. J. C **26**, 195 (2002).
- [21] A. Ali, V.M. Braun, and H. Simma, Z. Phys. C **63**, 437 (1994).
- [22] A. Ali and V.M. Braun, Phys. Lett. B **359**, 223 (1995).
- [23] P. Ball and V.M. Braun, Phys. Rev. D **58**, 094016 (1998).
- [24] S. Narison, Phys. Lett. B **327**, 354 (1994).
- [25] D. Melikhov and B. Stech, Phys. Rev. D **62**, 014006 (2000).
- [26] D. Becirevic, Flavor Physics and CP Violation (FPCP 2003) Conference, Paris, France, 2003.
- [27] B. Grinstein and D. Pirjol, Phys. Rev. D **62**, 093002 (2000).
- [28] M. Jamil Aslam, hep-ph/0604025, and references therein.